

# Effect of temperature on the mechanical properties of two polymeric geogrid materials

R. L. E. Desbrousses<sup>1</sup>, M. A. Meguid<sup>2</sup> and S. Bhat<sup>3</sup>

<sup>1</sup>PhD candidate, Department of Civil Engineering, McGill University, Montreal, QC, Canada,

E-mail: romaric.desbrousses@mail.mcgill.ca (corresponding author) (Orcid:0000-0001-5350-6812)

<sup>2</sup>Professor, Department of Civil Engineering, McGill University, Montreal, QC, Canada,

E-mail: mohamed.meguid@mcgill.ca (Orcid:0000-0002-5559-194X)

<sup>3</sup>Vice President, Global Business Development and Chief Technical Officer for Geosynthetics, Titan Environmental Containment Ltd., Ile des Chenes, Manitoba, Canada, E-mail: sam@titanenviro.ca

Received 16 June 2021, accepted 26 August 2021

**ABSTRACT:** Understanding the tensile behavior of geosynthetic reinforcement materials at different temperatures is essential for the design of reinforced soil structures in seasonally cold regions. This study describes a series of tensile tests performed on two polypropylene geogrid materials, namely a biaxial geogrid and a geogrid composite. A total of 84 tests were performed in an environmental chamber with temperatures as low as  $-30^{\circ}\text{C}$  and as high as  $+40^{\circ}\text{C}$ . The response of each material is examined over the range of investigated temperatures to evaluate the effect of temperature changes on the tensile strength of the two geogrid materials. The response of the biaxial geogrid is found to be sensitive to temperature variations, with samples tested at low temperatures exhibiting brittle behavior characterized by high rupture strength and small ultimate strain while samples tested at elevated temperatures displayed ductile behavior with large elongation at failure and comparatively small rupture strength. A similar response was found for the geogrid composite, however, the rupture strength seemed to be less sensitive to temperature changes. The modes of failure observed at each temperature are examined based on photographic evidence taken during the experiments.

**KEYWORDS:** Geosynthetics, geogrid, tensile loading, temperature effect, mechanical properties

**REFERENCE:** Desbrousses, R. L. E., Meguid, M. A. and Bhat, S. (2021). Effect of temperature on the mechanical properties of two polymeric geogrid materials. *Geosynthetics International*. [https://doi.org/10.1680/jgein.21.00032a]

## 1. INTRODUCTION

Geogrids are polymeric materials commonly used to reinforce and stabilize earth structures. They are typically made from three different types of polymers, – that is, polypropylene (PP), high-density polyethylene (HDPE), and polyester (PET). Polymeric materials used to manufacture geogrids are predominantly thermoplastics that exhibit a temperature-dependent behavior that ranges from being soft and flexible at high temperatures to brittle at low temperatures (McGown *et al.* 2004; Ward and Sweeney 2004; Koerner 2005). The temperature at which major changes occur in the mechanical properties of these materials is called the glass transition temperature ( $T_g$ ). Below its glass transition temperature, a polymeric material behaves in a rigid and brittle fashion while it becomes more rubbery when temperatures exceed  $T_g$  (Koerner *et al.* 1993; Jackson and Dhir 1996; McGown *et al.* 2004).

While geogrids are usually embedded within earth structures, the ambient temperature fluctuations

experienced by earth structures translate into temperature variations within the reinforcement layer (Segrestin and Jailloux 1988; Bush 1990; Zarnani *et al.* 2011). Segrestin and Jailloux (1988) developed a numerical model to evaluate the temperature change within a geosynthetics-reinforced earth structure as a result of seasonal temperature changes. They determined that outside temperature changes could be felt up to a depth of 10 m in earth structures and that geosynthetics were likely to experience temperature-induced changes in their mechanical properties (Segrestin and Jailloux 1988). This observation was echoed by Zarnani *et al.* (2011) and Kim and Kim (2020) who respectively studied the effects of soil temperature changes on geogrid strains placed in a reinforced embankment and in a geosynthetic-reinforced railway subgrade. Their respective findings revealed geogrid deformations are sensitive to soil temperature changes and geogrid strains increase with increasing soil temperature and decrease with decreasing temperature.

As shown in Table 1, several studies have been conducted to investigate the influence of temperature on

**Table 1. Summary of previous research on the effect of temperature on the mechanical properties of geosynthetics**

Author(s)	Year	Type of geosynthetic	Temperature range	Measured properties	Results
Calhoun	1972	PP Geotextile	-18°C to 82°C	• Tensile Strength	Tensile strength is not affected by temperature
Ariyama <i>et al.</i>	1997	PP Samples	25°C to 70°C	• Tensile Strength • Modulus of Elasticity	Tensile strength and modulus of elasticity decrease at elevated temperatures
Zornberg <i>et al.</i>	2004	PP Geotextile	24°C to 60°C	• Tensile Strength • Elongation	Higher temperatures lead to smaller tensile strengths and greater strains
Henry and Durell	2007	PP Geotextile	-54°C to 20°C	• Tensile Strength • Elongation • Puncture Strength	Tensile strength of dry geotextile decreased while that of wet geotextile increased with decreasing temperature. Lower ultimate strain at low temperature
Wang <i>et al.</i>	2008	HDPE Geogrid	-35°C to 20°C	• Creep • Strain	Smaller strains at lower temperatures
Kongkitkul <i>et al.</i>	2012	PP, PET, HDPE Geogrids	30°C to 50°C	• Tensile Strength • Elongation	Higher temperatures translate into lower tensile strain and greater ultimate strain. HDPE is the most sensitive to temperature changes, followed by PP and PET
Karademir and Frost	2014	PP Geotextile	20°C to 50°C	• Tensile Strength • Modulus of Elasticity • Stiffness	Reduction in tensile strength, modulus of elasticity, and stiffness with increasing temperature
Kasozi <i>et al.</i>	2014	HDPE Geogrid	30°C to 60°C	• Tensile Strength • Elongation	Greater temperatures lead to lower tensile strength and greater ultimate strain
Chantachot <i>et al.</i>	2016, 2017, 2018	HDPE and PP Geogrids	30°C to 50°C	• Tensile Strength • Elongation	PP, PET, and HDPE geogrids experience strength loss with increasing temperature. Only PP and PET geogrids exhibit greater strains
Bonthron & Jonsson	2017	PET and PP Geogrids	-20°C to 20°C	• Tensile Strength • Elongation	Geogrids become stiffer at low temperatures, developing a greater tensile strength and smaller ultimate strain
Koda <i>et al.</i>	2018	PP Geotextile	20°C to 80°C	• Tensile Strength • Elongation	Rise in temperature leads to smaller tensile strength and greater ultimate strain
Li <i>et al.</i>	2018	PP Samples	-30°C to 110°C	• Modulus of Elasticity	Modulus of elasticity is max at the lowest temperature and consistently decreases with increasing temperature

the mechanical properties of geosynthetics. Calhoun (1972) sought to determine how temperature affects the tensile strength of geotextiles and concluded that their strength is insensitive to temperature changes based on grab tensile tests on geotextiles performed at temperatures ranging from -18°C to 82°C. Zornberg *et al.* (2004) conducted a series of wide-width tensile tests on woven PP geotextiles at temperatures ranging from 24°C to 60°C. They reported that the geotextiles' tensile strength decreases while the ultimate strain increases with increasing temperature. Henry and Durell (2007) performed wide-width tensile and puncture tests on clean and moistened PP geotextiles at low temperatures and observed that the tensile strength of dry geotextiles decreases with decreasing temperature while that of wet geotextiles increases due to the stiffening effect of ice and soil fines present on the geotextile samples. They noted that both the dry and wet geotextiles elongate less at low temperatures and that a clear behavioral change occurs between 0°C and -20°C which corresponds to the range of  $T_g$  of polypropylene (Henry and Durell 2007).

Karademir and Frost (2014) subjected individual PP filaments taken from a needle-punched non-woven

geotextile to tensile tests at temperatures ranging from 20°C to 50°C. Their experiments revealed that increasing temperatures translate into reduced tensile strength, modulus of elasticity, stiffness, and yield strength. Additionally, Koda *et al.* (2018) performed wide-width tensile tests on a woven PP geotextile at 20°C, 50°C, and 80°C. They determined that a rise in temperature leads to a reduction in strength and an increase in ultimate strain, with the tensile strength at 80°C being 34% smaller than that at 20°C.

Analogous research efforts have been dedicated to investigating the temperature dependence of polymeric geogrids. Kongkitkul *et al.* (2012) performed tensile tests on PP, PET, and HDPE geogrids at temperatures ranging from 30°C to 50°C. They showed that geogrids experienced a reduction in tensile strength with increasing temperature and that HDPE geogrids were the most sensitive to temperature changes, followed by the PP and PET geogrids. Similarly, Chantachot *et al.* (2016, 2017, 2018) carried out tensile tests on uniaxial HDPE and biaxial PP geogrids (2016), on an HDPE geogrid (2017), and on PP, PET, and HDPE geogrids (2018) under increasingly high temperatures ranging from 30°C to

50°C. They demonstrated that an increase in temperature manifested itself in a greater ultimate strain in the PP geogrid while that of the HDPE geogrid remained unchanged. Kasozi *et al.* (2014) conducted tensile tests at elevated temperatures on a uniaxial HDPE geogrid in a bid to determine how a rise in temperature would affect its performance and reported that the HDPE geogrid loses strength with increasing temperature. Li *et al.* (2018) studied the temperature dependence of polypropylene by performing tensile tests on dog-bone PP samples at temperatures ranging from  $-30^{\circ}\text{C}$  to  $110^{\circ}\text{C}$  and indicated that the samples' modulus of elasticity decreases with increasing temperature. Additionally, Ariyama *et al.* (1997) showed that the modulus of elasticity and tensile strength of PP samples decrease at elevated temperatures after subjecting the samples to tensile tests at temperatures ranging from  $25^{\circ}\text{C}$  to  $70^{\circ}\text{C}$ .

An attempt to characterize the behavior of geogrids at low temperatures was made by Wang *et al.* (2008) who performed creep tests on a uniaxial HDPE geogrid over a temperature range of  $-35^{\circ}\text{C}$  to  $20^{\circ}\text{C}$  and observed that geogrids developed smaller strains at low temperatures. Likewise, Bonthron and Jonsson (2017) conducted tensile tests on one PET geogrid and four PP geogrids at temperatures ranging from  $-20^{\circ}\text{C}$  to  $20^{\circ}\text{C}$ . They concluded that geogrids generally become stiffer at low temperatures, exhibiting greater tensile strength and smaller ultimate strain compared to the reference temperature.

Geosynthetics have temperature-dependent properties and may exhibit a wide range of behavior depending on the temperatures they are exposed to (Bush 1990; Koerner *et al.* 1992; McGown *et al.* 2004; Cuelho *et al.* 2005; Han and Jiang 2013). As such, it is critical to characterize the mechanical behavior of geosynthetics over the range of temperatures they may be exposed to during their service life. The objective of this study is to investigate the effect of temperature on the tensile strength of a large aperture biaxial PP geogrid and biaxial PP geogrid composite, – that is, biaxial geogrid heat-bonded to a non-woven polyester geotextile, designed to reinforce ballasted railway embankments in seasonally cold regions (Bhat and Thomas 2015, 2017).

## 2. EXPERIMENTAL PROGRAM

This study aims to examine the effect of temperature on the tensile strength of a large aperture biaxial PP geogrid used to reinforce railway ballast and a biaxial PP geogrid composite designed to stabilize weak subgrades underlying railway ballast (see Figure 1).

Given the respective location of the two geosynthetics within the embankment and the wide range of temperatures railway embankments built in seasonally cold regions are exposed to (Liu *et al.* 2012; Desbrousses and Meguid 2021), tensile tests conducted at a single standard temperature may not yield results sufficient to characterize the tensile behavior of the geogrid and the geogrid composite over their full range of service temperatures. As

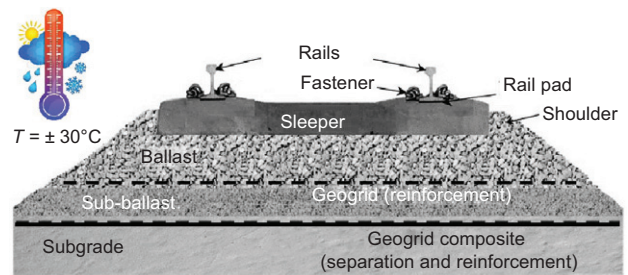


**Figure 1. Example of a typical installation of different reinforcement layers within a railway embankment**

such, a series of single-rib tensile tests are performed on single-rib samples of each material in accordance with Method A of ASTM D6637 (ASTM 2015) over a given range of temperatures. Tensile tests are conducted on single-rib samples of the biaxial PP geogrid at temperatures ranging from  $-30^{\circ}\text{C}$  to  $40^{\circ}\text{C}$  at  $10^{\circ}\text{C}$  increments while geogrid composite samples are exposed to testing temperatures ranging from  $-30^{\circ}\text{C}$  to  $20^{\circ}\text{C}$ . A total of six samples of each material are tested at each investigated temperature. It is noteworthy that the range of testing temperatures for the geogrid composite is kept between  $-30^{\circ}\text{C}$  and  $20^{\circ}\text{C}$  as the material is found to deform excessively at temperatures exceeding  $20^{\circ}\text{C}$ , leading to slippage between the sample and the test clamps.

### 2.1. Tested materials

Two types of geosynthetics used in railroad construction are tested in this study. The first is a large aperture biaxial polypropylene geogrid and the second is a biaxial polypropylene geogrid heat-bonded to a non-woven polyester geotextile. The properties of each material as reported by the manufacturer are given in Table 2 and are labeled as Machine Direction/Cross-Machine Direction. The biaxial PP geogrid and the geogrid composite are shown in Figures 2 and 3, respectively. Every sample used in this study was taken from the same roll of each material.

### 2.2. Testing equipment

The single-rib tensile tests were performed using an MTS Insight electromechanical testing system equipped with a

**Table 2. Minimum average roll value properties for the biaxial geogrid and biaxial geogrid composite (Titan Environmental Containment 2020, 2021)**

Property	Biaxial geogrid	Biaxial geogrid composite
Material	Polypropylene	Geogrid: Polypropylene Geotextile: Polyester
Ultimate Tensile Strength	30/30 kN/m	30/30 kN/m
Tensile Strength @ 2% Strain	11/11 kN/m	12/12 kN/m
Tensile Strength @ 5% Strain	21/21 kN/m	22/22 kN/m
Ribs/m	17	25
Aperture Size	57/57 mm	38/38 mm
Rib Thickness	1.8/1.2 mm	2.3/1.5 mm

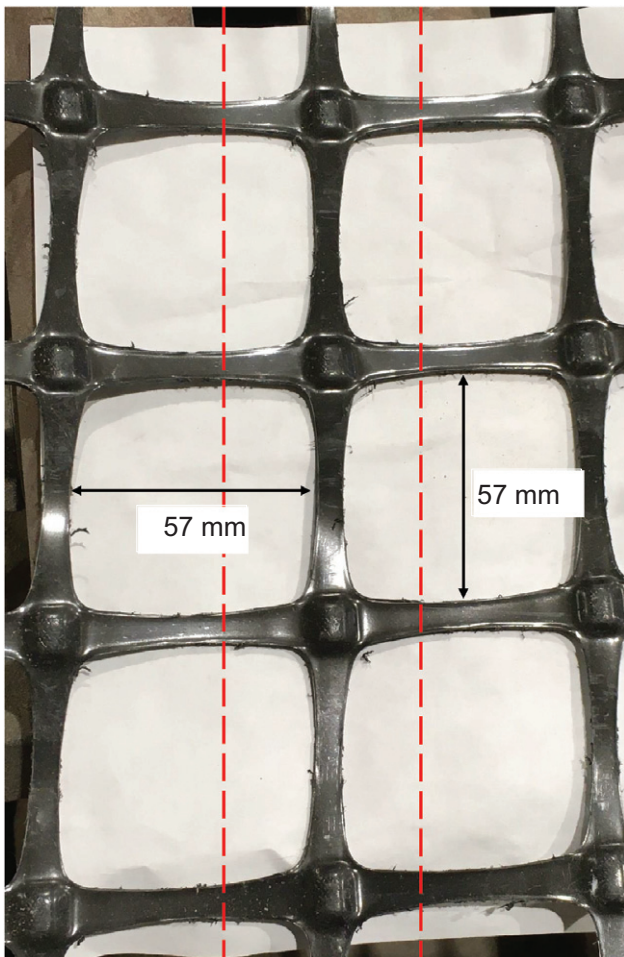


Figure 2. Large aperture biaxial pp geogrid

5 kN load cell. Wedge action grips with serrated jaws were used to clamp the single-rib samples during the experiments and were connected to the load frame by means of extension rods. To perform tensile tests at different temperatures, a temperature chamber was installed within the loading frame such that the grips and the tested samples could remain in a temperature-controlled environment throughout the tests. A schematic diagram and a photograph of the test setup are shown in Figure 4.

The temperature chamber used in this study was a Thermcraft medium-range laboratory oven with heating and cooling capabilities equipped with a heating system, a circulating air blower, a built-in thermocouple, and a cryogenic cooling system connected to a tank of liquid nitrogen. The circulating air blower operated at all times to ensure homogeneous temperature distribution within the chamber. The laboratory oven's temperature was controlled by an analog temperature controller connected to the oven's built-in thermocouple.

An MTS 632.11F-90 clip-on extensometer with a gauge length of 25 mm was used to monitor the sample elongation throughout the tests. It has a range of operating temperatures of  $-100^{\circ}\text{C}$  to  $150^{\circ}\text{C}$  and the variations in the calibration factor are negligible over the range of temperatures used in this study. The testing system was operated using the MTS Elite software suite.

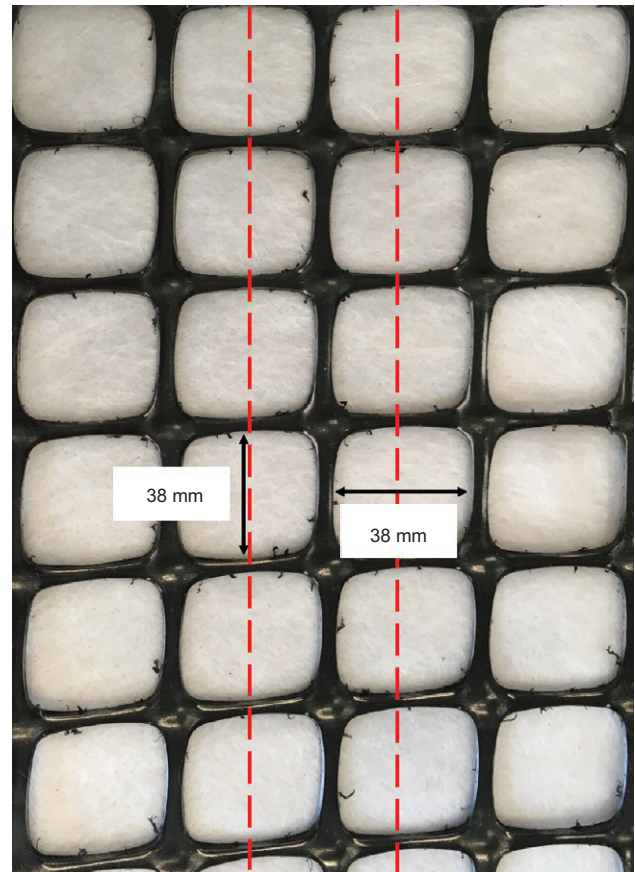


Figure 3. Biaxial geogrid composite

A thermocouple was taped to the surface of each sample and to one of the chamber's walls to monitor the temperature difference between the sample's surface and the chamber in real time. The time required for each sample to reach a stable initial temperature varied depending on the target temperature. Testing was initiated once the sample's surface temperature had reached the desired testing temperature.

### 3. TEST RESULTS AND DISCUSSION

#### 3.1. Biaxial geogrid

Figure 5 shows the average load-strain relationship measured for single ribs of the biaxial PP geogrid tested at temperatures that range from  $-30^{\circ}\text{C}$  to  $+40^{\circ}\text{C}$  with  $10^{\circ}\text{C}$  increments.

The geogrid was first tested at a reference temperature of  $20^{\circ}\text{C}$  as prescribed by ASTM D6637 to establish a set of reference properties and compare them to the values reported by the manufacturer. A mean ultimate tensile strength of  $33.54\text{ kN/m}$  was obtained and compares well with the minimum average roll value (MARV) ultimate tensile strength of  $30.00\text{ kN/m}$  reported by the manufacturer as shown in Table 2.

The load-strain curves in Figure 5 indicate that the geogrid's tensile behavior is temperature-sensitive. At room temperature ( $+20^{\circ}\text{C}$ ), the tested sample reached an ultimate load of  $33.6\text{ kN/m}$  at about 14% strain.

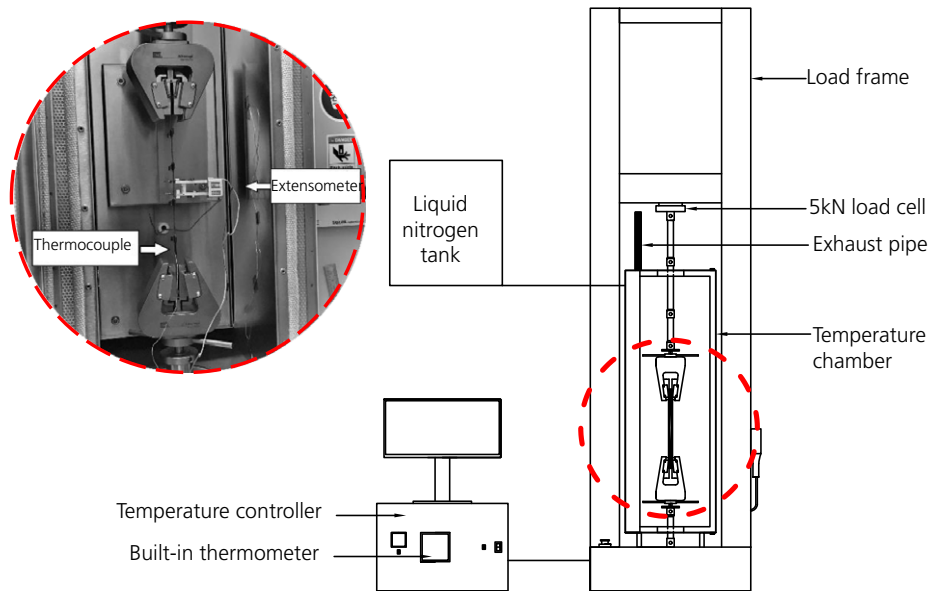


Figure 4. Diagram of the test set up used to perform tensile tests in a temperature-controlled environment

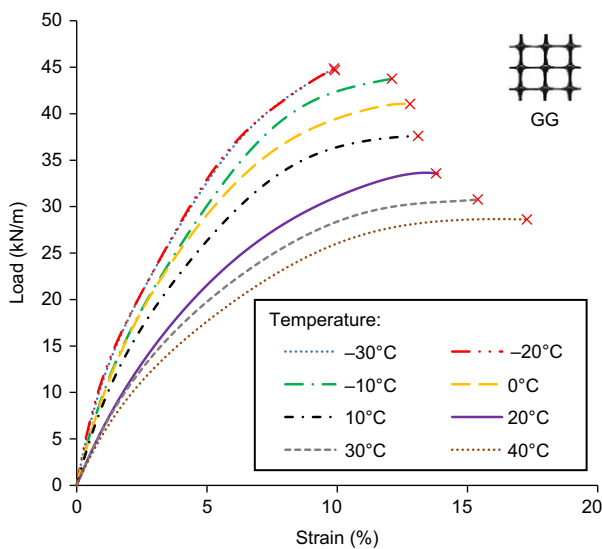


Figure 5. Average load-strain relationship for the geogrid at temperatures ranging from -30°C to 40°C

When the temperature increases above 20°C, the load-strain relationships retain a shape akin to that at the reference temperature but display markedly lower rupture strengths and greater ultimate strains. The initial slope of the load-strain curves at elevated temperatures is also noticeably lower than the one at the reference temperature, suggesting that the geogrid loses stiffness at higher temperatures. Conversely, the load-strain relationships at temperatures below 20°C occupy the upper part of the plot and exhibit increasingly greater rupture strengths and smaller ultimate strains as the temperature decreases. The initial slope of the load-strain curves at low temperatures is greater than that at 20°C, hinting at a stiffer geogrid response to tensile loads with decreasing temperature. The ultimate strength was found to incrementally increase to 37.6, 41, 43.7, and 44.7 kN/m when the temperature decreased from +20°C to +10, 0, -10, and -20. It is

noteworthy that the load-strain relationships at -20°C and -30°C are almost identical.

### 3.1.1. Effect of temperature on the strength at failure

The average rupture strengths at each investigated temperature are summarized in Table 3 and normalized against the rupture strength at 20°C in Figure 6. The results demonstrate that temperature has a notable effect on the rupture strength of the tested geogrid. Low temperatures generally translate into high rupture strengths compared to that at the reference temperature and geogrids exposed to high temperatures experience a strength loss. Over the range of tested temperature, the maximum increase in rupture strength occurred at -30°C where the reported tensile strength was about 33.7% greater than the reference value. Conversely, the maximum decrease in tensile strength happened at 40°C where the maximum tensile strength mobilized by the geogrid was about 14.8% smaller than the reference value. Figure 6 reveals that the rate of change in tensile strength is not constant throughout the range of tested temperatures. Indeed, the rupture strength seems to increase almost linearly from 40°C to -10°C, but the rate of change in strength decreases significantly between -10°C and -20°C and becomes almost non-existent between -20°C and -30°C with the

Table 3. Temperature-induced changes in rupture strength ( $T_{ult}$ )

Temperature (°C)	$T_{ult}$ (kN/m)	% Change
-30	44.85	33.69
-20	44.69	33.21
-10	43.76	30.46
0	41.03	22.29
10	37.58	12.03
20	33.55	0.00
30	30.77	-8.29
40	28.60	-14.76

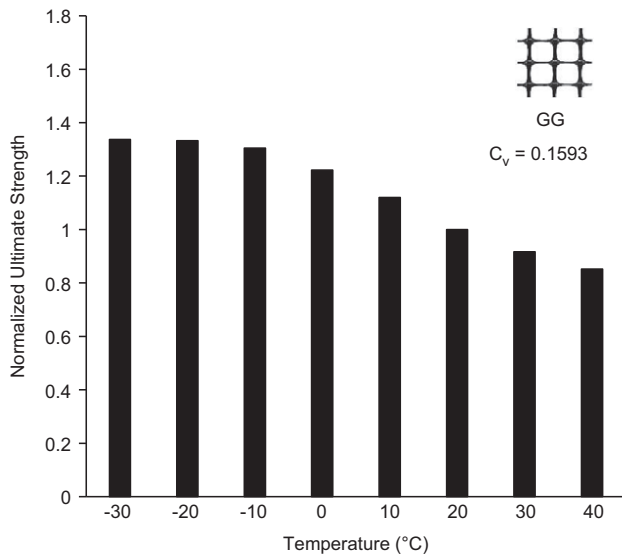


Figure 6. Effect of temperature on the normalized rupture strength of the geogrid ( $T_{ult}/T_{ult@20}$ )

rupture strength at  $-30^{\circ}\text{C}$  being only 0.36% greater than the one at  $-20^{\circ}\text{C}$ . This suggests that an important transition occurs in the geogrid's behavior around  $-10^{\circ}\text{C}$ . This could be attributed to reaching polypropylene's glass transition temperature, which is usually between  $0^{\circ}\text{C}$  and  $-20^{\circ}\text{C}$  (Henry and Durell 2007). A similar phenomenon was observed by Henry and Durell (2007) who performed wide-width tensile tests on PP geotextiles at low temperatures and noticed a clear change in the geotextile's behavior between  $0^{\circ}\text{C}$  and  $-20^{\circ}\text{C}$ .

Linear and polynomial regression were performed to characterize the relationship between the geogrid's normalized tensile strength and temperature in terms of the temperature effect parameter  $A^f$  as defined in Kongkitkul *et al.* (2012) and Chantachot *et al.* (2018).  $A^f$  is the ratio between the rupture strength ( $T_{ult}$ ) at a given temperature and the rupture strength ( $T_{ult@20^{\circ}\text{C}}$ ) at the reference temperature. The relationship between the normalized rupture strength and temperature from  $-10^{\circ}\text{C}$  to  $40^{\circ}\text{C}$  was successfully described using a linear equation (Equation 1). However, the relationship between  $-30^{\circ}\text{C}$  and  $-10^{\circ}\text{C}$  was more adequately represented using a quadratic expression (Equation 2). The temperature effect parameter  $A^f$  is given by the following equations and summarized in Figure 7 in which the solid curves refer to the experimental data while the dashed ones represent Equations 1 and 2.

For  $-10^{\circ}\text{C} < T < 40^{\circ}\text{C}$ :

$$\frac{T_{ult}}{T_{ult@20}} = A^f = -0.00942 \times T[^{\circ}\text{C}] + 1.21092 \quad (1)$$

For  $-30^{\circ}\text{C} < T < -10^{\circ}\text{C}$ :

$$\begin{aligned} \frac{T_{ult}}{T_{ult@20}} = A^f &= \\ &= -0.00011 \times T[^{\circ}\text{C}]^2 - 0.00617 \times T[^{\circ}\text{C}] \\ &\quad + 1.25423 \end{aligned} \quad (2)$$

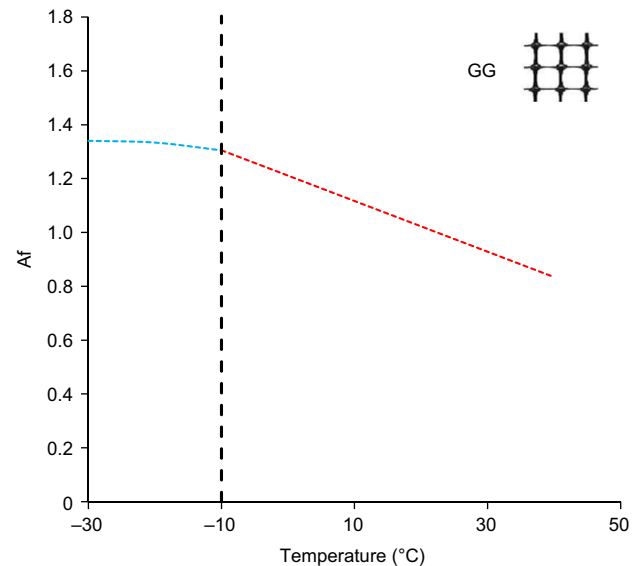


Figure 7. (a) Normalized rupture strength of the geogrid vs. temperature, (b)  $A^f$  from  $-10^{\circ}\text{C}$  to  $40^{\circ}\text{C}$ , (c)  $A^f$  from  $-30^{\circ}\text{C}$  to  $-10^{\circ}\text{C}$ , (d)  $A^f$  over the range of investigated temperatures

To quantify the effect of temperature on the geogrid's stiffness, the tensile strength at 2% strain of the geogrid at each temperature is normalized against a reference value obtained at  $20^{\circ}\text{C}$  and is plotted in Figure 8. The tensile strength mobilized at 2% strain considerably increased at temperatures below  $20^{\circ}\text{C}$  and experienced a reduction at temperatures exceeding  $20^{\circ}\text{C}$ , demonstrating that for the same displacement, the geogrid developed greater tensile stress values at low temperatures, which emphasizes the increasingly brittle response of the material with decreasing temperature.

### 3.1.2. Effect of temperature on the ultimate strain

Figure 9 shows the variations in normalized ultimate strain with changes in temperature. The normalized

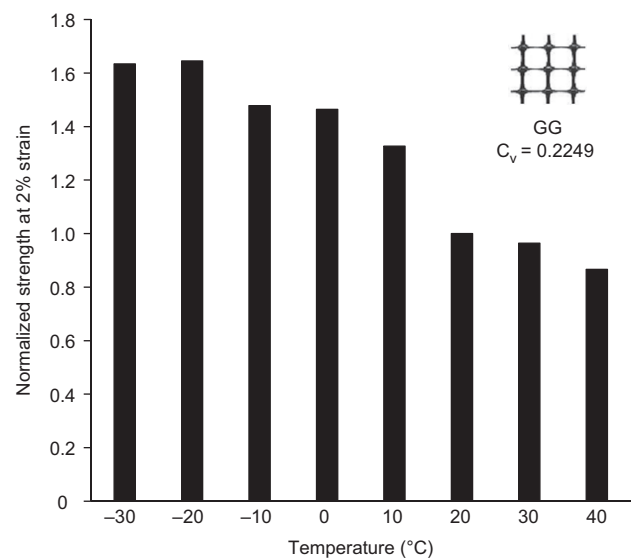
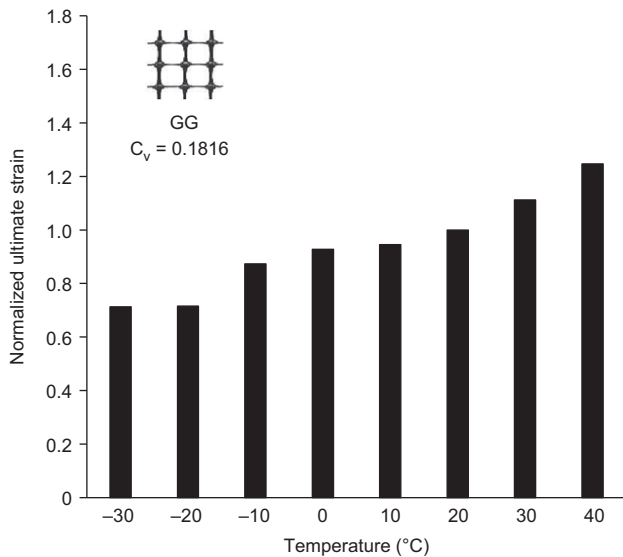


Figure 8. Effect of temperature on the normalized tensile strength of the geogrid at 2% strain ( $T_{2\%}/T_{2\%@20}$ )



**Figure 9.** Variations in normalized ultimate strain with temperature for the geogrid material

ultimate strain is obtained by dividing the ultimate strain at a given temperature by the strain at the reference temperature, – that is, 20°C. The ultimate strain follows a trend opposite to that of the rupture strength, with its value increasing with an increase in temperature. The minimum ultimate strain occurs at –30°C and the maximum is at 40°C, with the strain at 40°C being almost 75% greater than the one at –30°C. It is noteworthy that the ultimate strain at –30°C and –20°C are found to be very similar and that a substantial strain increase occurs at –10°C, further confirming the

observation that considerable behavioral changes take place in the geogrid at that temperature. The rate of strain increase between –10°C and 10°C is relatively low but picks up considerably from 10°C to 40°C. The changes in ultimate strain along with the observed differences in tensile strength at each temperature demonstrate that the geogrid becomes more ductile at elevated temperatures and loses some of its load-carrying capacity and that the reverse occurs at lower temperatures, where the geogrid's behavior is characterized by a stiff and brittle response to tensile loads.

### 3.1.3. Failure patterns

Testing the PP geogrid at temperatures ranging from –30°C to 40°C revealed that the material exhibits not only changing mechanical properties but also different modes of failure as temperatures vary. In every tensile test, failure happened as one of the junctions within the test gauge length broke. Figures 10a–10f show the various failure modes of the geogrid's junctions at different temperatures. At 20°C (Figure 10d), the junction split in half after the single-rib sample had experienced plastic deformation. As the temperature was increased to 30°C and 40°C (Figures 10e and 10f, respectively), the geogrid became more ductile and elongated more before failing. This additional ductility meant that the material behaved in a more viscous manner, with the junctions exhibiting significant distortion at failure. However, no particular damage was observed in the ribs neighboring the failed junction. At lower temperatures, the geogrid became stiffer and gradually lost its ability to elongate when subjected to tensile loads. At 0°C, the single-rib samples deformed significantly less than at 20°C and exhibited a more brittle

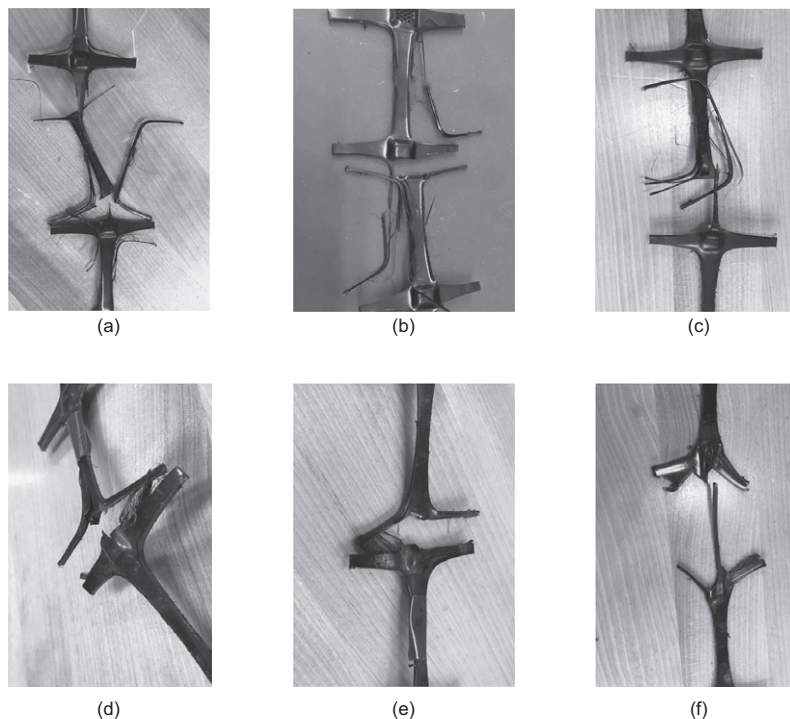


**Figure 10.** Failure modes of the geogrid at (a) –30°C, (b) –10°C, (c) 0°C, (d) 20°C, (e) 30°C, and (f) 40°C

and sudden failure. The samples started to have what seemed to be fibers popping out of the sides of their ribs when the tensile load increased up to failure. A similar phenomenon was observed at  $-10^{\circ}\text{C}$  and  $-30^{\circ}\text{C}$  (Figures 10a and 10b respectively), with the failure becoming even more brittle and sudden with more fibers crumbling from the sides of the single rib samples as the temperature was decreased.

The observed failure patterns along with the recorded load-displacement responses coincide with the transition from ductile to brittle behavior that occurs when the temperature drops below polypropylene's glass transition temperature ( $T_g$ ). Polypropylene being a semi-crystalline thermoplastic, its molecules have a very limited ability to reorient themselves at temperatures below its  $T_g$ , giving it a hard and brittle behavior akin to that the geogrid displayed between  $-30^{\circ}\text{C}$  to  $-10^{\circ}\text{C}$  characterized by high tensile strength, low ultimate strain, and relatively negligible junction deformation along with fiber spalling at failure. On the other hand, once polypropylene is exposed to temperatures exceeding its  $T_g$ , its molecules have a greater ability to reorient themselves, giving it a more flexible and ductile behavior similar to that of the geogrid between  $0^{\circ}\text{C}$  and  $40^{\circ}\text{C}$ .

### 3.2. Biaxial PP geogrid composite

Figure 11 shows the average load-strain relationships obtained from tensile load tests performed on the geogrid composite at temperatures ranging from  $-30^{\circ}\text{C}$  to  $20^{\circ}\text{C}$ . The average load-strain relationships indicate that the ultimate strain is sensitive to temperature variations, with samples tested at low temperatures exhibiting a significantly lower strain at failure than samples tested at higher temperatures. The rupture strength however seems to be relatively insensitive to temperature changes, with only minor strength variations being observed over the range of tested temperatures. The general shape of the load-strain curves shows that the geogrid composite develops a more

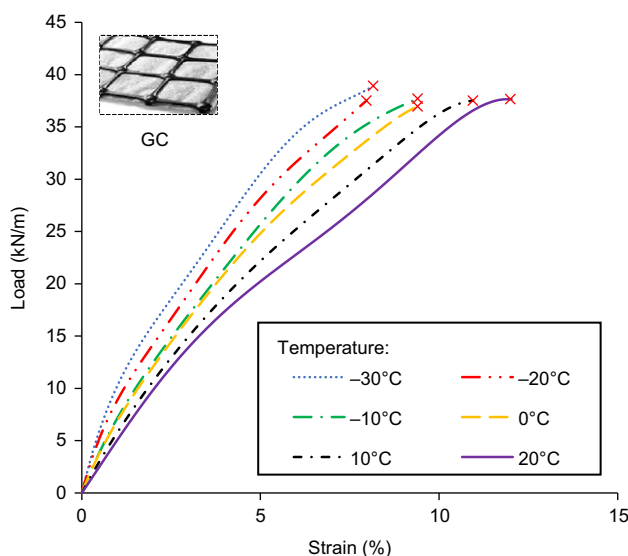


Figure 11. Average load-strain relationships for the geogrid composite at different temperatures

brittle response to tensile loads as the surrounding temperature decreases. The single-rib tensile tests performed at the reference temperature recommended by ASTM D6637, – that is,  $20^{\circ}\text{C}$ , gave a mean ultimate tensile strength of  $37.59\text{ kN/m}$  which is in good agreement with the MARV ultimate tensile strength of  $30.00\text{ kN/m}$  reported by the manufacturer. The geogrid composite was tested in an effort to characterize its overall load-displacement response at various temperatures. The recorded variations of ultimate tensile strength and strain suggest its composite nature leads to a load-displacement response that is dissimilar to that of the PP geogrid alone.

#### 3.2.1. Effect of temperature on the tensile strength at failure

The changes in normalized rupture strength with temperature are depicted in Figure 12 and the rupture strength at each temperature along with the percentage change in strength with respect to the reference temperature are listed in Table 4. Contrary to the trend observed with the biaxial PP geogrid, the investigated geogrid composite shows insignificant temperature-induced changes in rupture strength, with maximum difference occurring at  $-30^{\circ}\text{C}$  where the rupture strength is found to be about 3.4% smaller than at  $20^{\circ}\text{C}$ . The rupture strength remained relatively constant over the entire range of the investigated

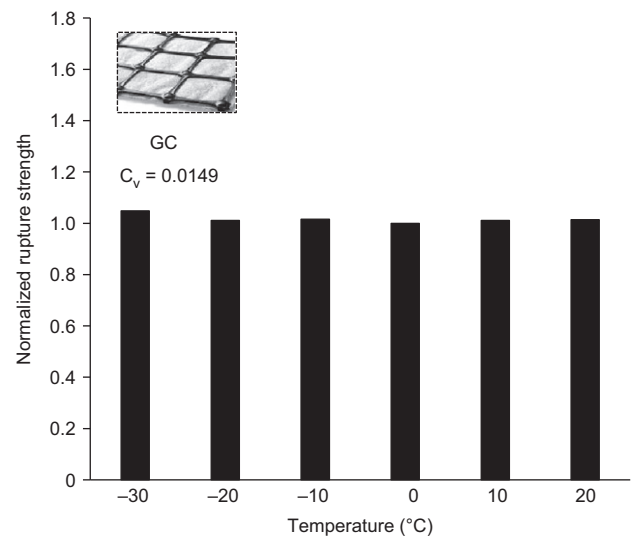


Figure 12. Normalized rupture strength of the geogrid composites at each tested temperature

Table 4. Rupture strength ( $T_{ult}$ ) at temperatures ranging from  $-30^{\circ}\text{C}$  to  $20^{\circ}\text{C}$

Temperature ( $^{\circ}\text{C}$ )	$T_{ult}$ (kN)	% Change
-30	38.91	3.38
-20	37.52	-0.32
-10	37.70	0.16
0	37.11	-1.41
10	37.51	-0.36
20	37.64	0.00

temperatures. This may be attributed to the geogrid being heat bonded to a polyester geotextile.

The bond between the geogrid and the geotextile allows for the tensile strength of both materials to be simultaneously mobilized. Jeon (2016) indicated that when a geogrid composite is subjected to tensile load, the geogrid tends to fail before the geotextile as observed in the geogrid composite used in this study. Given that the tensile strength of the large aperture biaxial geogrid described in the previous section exhibited a clear temperature-dependent response, it is expected that a load transfer mechanism develops through the bond between the geogrid and the non-woven polyester geotextile which prevents the geogrid from developing greater tensile strengths at low temperatures. However, the geogrid composite still fails at smaller strains at low temperatures due to the geogrid's increasingly brittle behavior.

Additionally, Figure 13 shows the variations in the composite's normalized tensile strength at 2% strain with temperature. The mobilized tensile strain continually increased as the temperature decreased, indicating an increasingly stiff response of the geogrid composite at cold temperatures.

### 3.2.2. Effect of temperature on the ultimate strain

Figure 14 shows the sensitivity of the normalized strain to changes in temperature. While it was previously observed that the geogrid composite's rupture strength was relatively insensitive to temperature, the material exhibits markedly different elongation properties at different temperatures. The samples tested at 20°C had the highest strain at failure amongst all tested samples. Decreasing temperatures had the effect of reducing the material's ability to deform under increasing tensile load. The lowest strains were recorded at -20°C and -30°C. The smallest strain was 33.7% smaller than the one at 20°C.

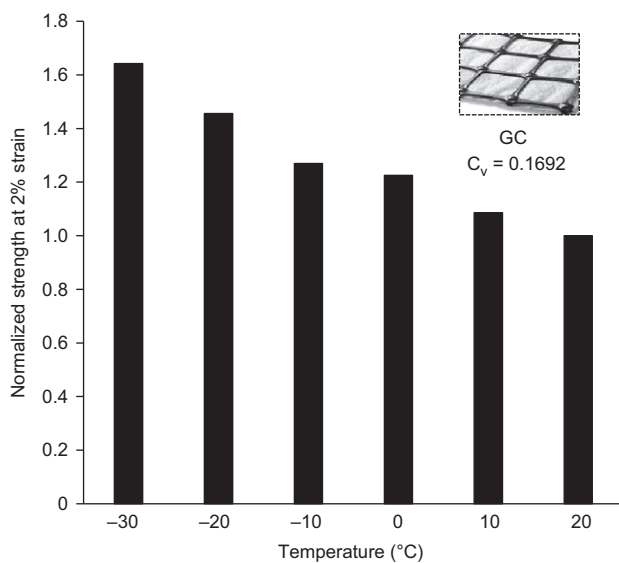


Figure 13. Normalized tensile strength of the geogrid composite at 2% strain at each tested temperature

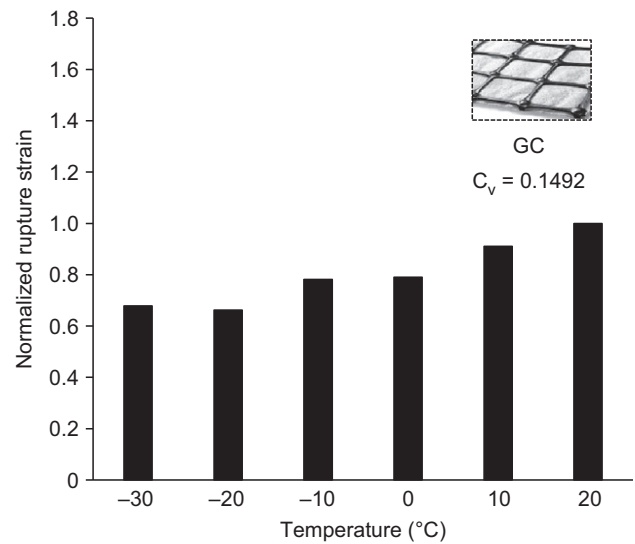


Figure 14. Normalized ultimate strain of the geogrid composite at temperatures ranging from -30°C to 20°C

### 3.2.3. Failure modes

Figures 15a–15f show the different junction failure patterns observed at every tested temperature for the geogrid composite. Every tensile test conducted during this experimental campaign ended with failure of a geogrid junction within the test gauge length. At the reference temperature (Figure 15f), the junction failed by splitting and little damage was observed in the rest of the sample. Similar behavior was also observed at 10°C (Figure 15e). However, at lower temperatures, as the material became more brittle, the junction failed more suddenly, and the rest of the sample appeared to sustain damage during testing by having fibers popping out of the ribs' sides. The fibrous appearance of the failed samples became increasingly clear with decreasing temperature as demonstrated by Figures 15a–15d. The evolution of failure patterns with temperature echoes the findings of Section 3.1.3 whereby the samples tested at low temperatures ranging from -30°C to -10°C exhibited considerably smaller ultimate strains (see Figure 12) and significant fiber spalling along their ribs compared to samples tested at 10°C and 20°C. This emphasizes the behavioral transition that takes place when the testing temperature exceeds the PP geogrid's  $T_g$  as the material becomes increasingly able to deform under loads.

## 4. CONCLUSIONS

The goal of this study was to investigate the effect of temperature on the mechanical properties of a large aperture biaxial PP geogrid and a biaxial PP geogrid composite used to reinforce and stabilize ballasted railway embankments in seasonally cold regions. The major conclusions drawn from the current study are as follows:

- The ultimate tensile strength and strain of the biaxial PP geogrid were found to be sensitive to temperature changes. A rise in temperature beyond the reference

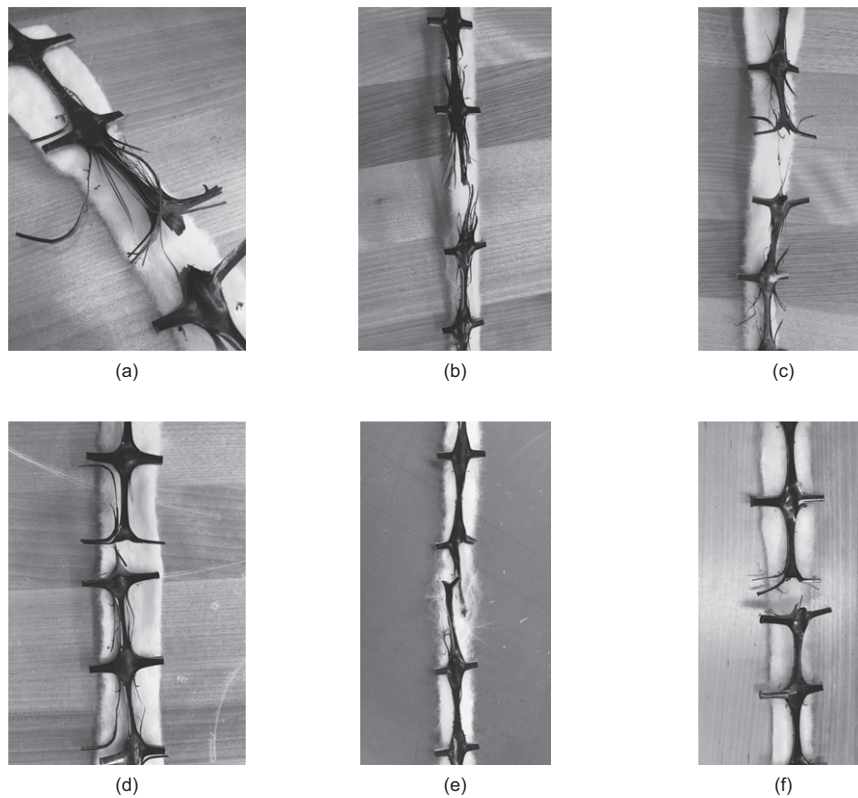


Figure 15. Failure modes for the geogrid composite at (a)  $-30^{\circ}\text{C}$ , (b)  $-20^{\circ}\text{C}$ , (c)  $-10^{\circ}\text{C}$ , (d)  $0^{\circ}\text{C}$ , (e)  $10^{\circ}\text{C}$ , and (f)  $20^{\circ}\text{C}$

- value ( $20^{\circ}\text{C}$ ) resulted in a reduction in tensile strength and a rise in ultimate strain, while smaller ultimate strains and greater tensile strengths were observed as the temperatures were lower below  $20^{\circ}\text{C}$ . The maximum ultimate strain was recorded at  $40^{\circ}\text{C}$  with a value of about 17% along with the minimum tensile strength which was about 15% smaller than the reference one. Conversely, the smallest ultimate strain (about 10%) occurred at  $-30^{\circ}\text{C}$  along with the maximum tensile strength which was about 34% greater than the one measured at  $20^{\circ}\text{C}$ .
- A pronounced transition in the biaxial PP geogrid's response to tensile loads was observed at temperatures below  $-10^{\circ}\text{C}$ . The rupture strength increased almost linearly between  $-10^{\circ}\text{C}$  and  $40^{\circ}\text{C}$  but varied insignificantly between  $-20^{\circ}\text{C}$  and  $-30^{\circ}\text{C}$ . The ultimate strain exhibited a similar trend, with only minor changes being reported between  $-20^{\circ}\text{C}$  and  $-30^{\circ}\text{C}$ . Such behavioral changes may be attributed to the testing temperature dipping below the glass transition temperature of polypropylene and the corresponding transition from ductile to brittle behaviour.
  - The ultimate tensile strength of the geogrid composite was relatively insensitive to temperature changes while its ultimate strain decreased with the decrease in temperature. The maximum ultimate strain was recorded at  $20^{\circ}\text{C}$  with a value of 12.0% while the minimum ultimate strain occurred at  $-30^{\circ}\text{C}$  with a value of 8.2%

- The responses of both the biaxial PP geogrid and biaxial PP geogrid composite to tensile loads were considerably affected by temperature variations, indicating that properties determined by standard tests performed at room temperature do not capture the full extent of a polymeric material's range of tensile behavior. Geogrids destined to be placed in earth structures constructed in regions known to have distinct and pronounced seasonal climatic changes should be tested over a range of temperatures representative of those they would be exposed to during their service life.
- Additional tests are needed to quantify the individual effect of the geogrid and geotextile on the mechanical behavior of the geogrid composite.

## ACKNOWLEDGMENTS

This research is funded by NSERC and McGill University. The authors are grateful to their industrial partner, Titan Environmental Containment Ltd., for supplying the geogrid material and providing technical support for this project. We would like to thank P. Hubert of McGill University for providing access to the environmental chamber required for the reported experiments.

## ABBREVIATIONS

GC	geocomposite
GG	geogrid
PP	polypropylene

## REFERENCES

- Ariyama, T., Mori, Y. & Kaneko, K. (1997). Tensile properties and stress relaxation of polypropylene at elevated temperatures. *Polymer Engineering & Science*, **37**, No. 1, 81–90, <https://doi.org/10.1002/pen.11647>.
- ASTM (2015). ASTM D6637/D6637M-15, Standard test method for determining tensile properties of geogrids by the single or multi-rib tensile method. ASTM, pp. 435–440, [https://doi.org/10.1520/D6637\\_D6637M-15](https://doi.org/10.1520/D6637_D6637M-15).
- Bhat, S. & Thomas, J. (2015). Design and construction of a geosynthetic reinforced pavement on weak subgrade. In *Canadian Geotechnical Conference & Canadian Permafrost Conference*, Canadian Geotechnical Society, Quebec City, QC, Canada, pp. 1–5.
- Bhat, S. & Tomas, J. (2017). Railroad subgrade stabilization using biaxial geogrid-geotextile composite – a case study. In *First International Conference on Technology and Application of Geotextiles*, Paredes, L., Gourc, J. P., Valdebenito, V., Mondaca, W. & Binignat, C., Editors, Gecamin, Santiago, Chile, pp. 1–7.
- Bonthron, B. & Jonsson, C. (2017). *Geogrids in Cold Climate*, Lulea University of Technology, Lulea, Sweden.
- Bush, D. I. (1990). Variation of long-term design strength of geosynthetics in temperatures up to 40°C. In *Proceedings of the Fourth International Conference on Geotextiles, Geomembranes, and Related Products*, Balkema, The Hague, The Netherlands, pp. 673–676.
- Calhoun, C. C. (1972). *Development of Design Criteria and Acceptance Specifications for Plastic Filter Cloths*, US Army Engineer Waterways Experiment Station, Vicksburg, MS, USA.
- Chantachot, T., Kongkitkul, W. & Tatsuoka, F. (2016). Load-strain-time behaviours of two polymer geogrids affected by temperature. *International Journal of GEOMATE*, **10**, No. 3, 1869–1876, <https://doi.org/10.21660/2016.21.5192>.
- Chantachot, T., Kongkitkul, W. & Tatsuoka, F. (2017). Effects of temperature on elastic stiffness of a HDPE geogrid and its model simulation. *International Journal of GEOMATE*, **12**, No. 32, 94–100, <https://doi.org/10.21660/2017.32.6620>.
- Chantachot, T., Kongkitkul, W. & Tatsuoka, F. (2018). Effects of temperature rise on load-strain-time behaviour of geogrids and simulations. *Geosynthetics International*, **25**, No. 3, 287–303, <https://doi.org/10.1680/jgein.18.00008>.
- Cuelho, E. V., Perkins, S. W. & Ganeshan, S. K. (2005). Determining geosynthetic material properties pertinent to reinforced pavement design. In *Advances in Pavement Engineering*, Schwartz, C. W., Tutumluer, E. & Tashman, L. Editors, American Society of Civil Engineers, Austin, TX, USA, pp. 1–12, [https://doi.org/10.1061/40776\(155\)19](https://doi.org/10.1061/40776(155)19).
- Desbrousses, R. L. E. & Meguid, M. (2021). On the analysis and design of reinforced railway embankments in cold climate: a review. In *CSCE 2021 Annual Conference*, Tighe, S., Walbridge, S. & Henderson, V. Editors, Springer, Niagara Falls, ON, Canada, pp. 588–598.
- Han, J. & Jiang, Y. (2013). Use of geosynthetics for performance enhancement of earth structures in cold regions. *Sciences in Cold and Arid Regions*, **5**, No. 5, 517, <https://doi.org/10.3724/SP.J.1226.2013.00517>.
- Henry, K. S. & Durell, G. R. (2007). Cold temperature testing of geotextiles: new, and containing soil fines and moisture. *Geosynthetics International*, **14**, No. 5, 320–329, <https://doi.org/10.1680/gein.2007.14.5.320>.
- Jackson, N. & Dhir, R. K. (1996). *Civil Engineering Materials*, 5th edn. Palgrave MacMillan, Basingstoke, UK.
- Jeon, H.-Y. (2016). Geotextile composites having multiple functions. In *Geotextiles: From Design to Applications*, Koerner, R. M., Editor, Elsevier, Duxford, UK, pp. 413–425, <https://doi.org/10.1016/B978-0-08-100221-6.00018-8>.
- Karademir, T. & Frost, J. D. (2014). Micro-scale tensile properties of single geotextile polypropylene filaments at elevated temperatures. *Geotextiles and Geomembranes*, **42**, No. 3, 201–213, <https://doi.org/10.1016/j.geotextmem.2014.03.001>.
- Kasozi, A. M., Siddharthan, R. V. & Mahamud, R. (2014). MSE wall geogrid tensile strength at high temperature sites. *Environmental Geotechnics*, **3**, No. 1, 4–16, <https://doi.org/10.1680/envgeo.13.00073>.
- Kim, U. J. & Kim, D. S. (2020). Load sharing characteristics of rigid facing walls with geogrid reinforced railway subgrade during and after construction. *Geotextiles and Geomembranes*, **48**, No. 6, 940–949, <https://doi.org/10.1016/j.geotextmem.2020.08.002>.
- Koda, E., Miszkowska, A. & Kiersnowska, A. (2018). Assessment of the temperature influence on the tensile strength and elongation of woven geotextiles used in landfill. In *11th International Conference on Geosynthetics 2018, ICG 2018*, Korean Geosynthetics Society, Editors, International Geosynthetics Society, Seoul, Korea, vol. 4, pp. 2676–2681.
- Koerner, R. M. (2005). *Designing with Geosynthetics*, 5th edn. Pearson Education, Upper Saddle River, NJ, USA.
- Koerner, R. M., Lord, A. E. & Hsuan, Y. H. (1992). Arrhenius modeling to predict geosynthetic degradation. *Geotextiles and Geomembranes*, **11**, No. 2, 151–183, [https://doi.org/10.1016/0266-1144\(92\)90042-9](https://doi.org/10.1016/0266-1144(92)90042-9).
- Koerner, R. M., Hsuan, Y. & Lord, A. E. (1993). Remaining technical barriers to obtaining general acceptance of geosynthetics. *Geotextiles and Geomembranes*, **12**, No. 1, 1–52, [https://doi.org/10.1016/0266-1144\(93\)90035-M](https://doi.org/10.1016/0266-1144(93)90035-M).
- Kongkitkul, W., Tabsombut, W., Jaturapitakkul, C. & Tatsuoka, F. (2012). Effects of temperature on the rupture strength and elastic stiffness of geogrids. *Geosynthetics International*, **19**, No. 2, 106–123, <https://doi.org/10.1680/gein.2012.19.2.106>.
- Li, G., Li, J., Wang, J., Feng, J., Guo, Q., Zhou, J. & Mitrouchev, P. (2018). The effect of temperature on mechanical properties of polypropylene. In *Advanced Manufacturing and Automation VII. IWAMA 2017. Lecture Notes in Electrical Engineering*, Wang, K., Wang, Y., Strandhagen, J. and Yu, T., Editors, Springer, Changshu, China, vol. 451, pp. 143–149, [https://doi.org/10.1007/978-981-10-5768-7\\_14](https://doi.org/10.1007/978-981-10-5768-7_14).
- Liu, H., Niu, F., Niu, Y., Lin, Z., Lu, J. & Luo, J. (2012). Experimental and numerical investigation on temperature characteristics of high-speed railway's embankment in seasonal frozen regions. *Cold Regions Science and Technology*, **81**, 55–64, <https://doi.org/10.1016/j.coldregions.2012.04.004>.
- McGown, A., Khan, A. J. & Kupec, J. (2004). The isochronous strain energy approach applied to the load–strain–time–temperature behaviour of geosynthetics. *Geosynthetics International*, **11**, No. 2, 114–130, <https://doi.org/10.1680/gein.2004.11.2.114>.
- Segrestin, P. & Jailloux, J. M. (1988). Temperature in soils and its effect on the ageing of synthetic materials. *Geotextiles and Geomembranes*, **7**, No. 1–2, 51–69, [https://doi.org/10.1016/0266-1144\(88\)90018-0](https://doi.org/10.1016/0266-1144(88)90018-0).
- Titan Environmental Containment (2020). *Titan Rail Grid 30 (Issue November)*. Titna Environmental Containment, Iles des Chenes, Manitoba, Canada.
- Titan Environmental Containment (2021). *Swamp Grid 30 (Issue January)*, Titna Environmental Containment City, Iles des Chenes, Manitoba, Canada.
- Wang, E. L., Xu, E. L., Zhang, B., Zhong, H., Gao, Z. K. & Chang, J. D. (2008). Experimental study on creep properties of plastic geogrid under low temperature. In *Geosynthetics in Civil and Environmental Engineering - Geosynthetics Asia 2008: Proceedings of the 4th Asian Regional Conference on Geosynthetics*, Li, G., Chen, Y. & Tang, X. Editors, Springer, Shanghai, China, pp. 70–73, [https://doi.org/10.1007/978-3-540-69313-0\\_15](https://doi.org/10.1007/978-3-540-69313-0_15).
- Ward, I. M. & Sweeney, J. (2004). *An Introduction to the Mechanical Properties of Solid Polymers*, 2nd edn. John Wiley & Sons Ltd, Chichester, UK.
- Zarnani, S., Scott, J. D. & Sego, D. C. (2011). Effect of soil temperature changes on geogrid strains. *Canadian Geotechnical Journal*, **48**, No. 8, 1287–1294, <https://doi.org/10.1139/t11-035>.
- Zornberg, J. G., Byler, B. R. & Knudsen, J. W. (2004). Creep of geotextiles using time–temperature superposition methods. *Journal of Geotechnical and Geoenvironmental Engineering*, **130**, No. 11, 1158–1168, [https://doi.org/10.1061/\(ASCE\)1090-0241\(2004\)130](https://doi.org/10.1061/(ASCE)1090-0241(2004)130).

The Editor welcomes discussion on all papers published in *Geosynthetics International*. Please email your contribution to [discussion@geosynthetics-international.com](mailto:discussion@geosynthetics-international.com)